

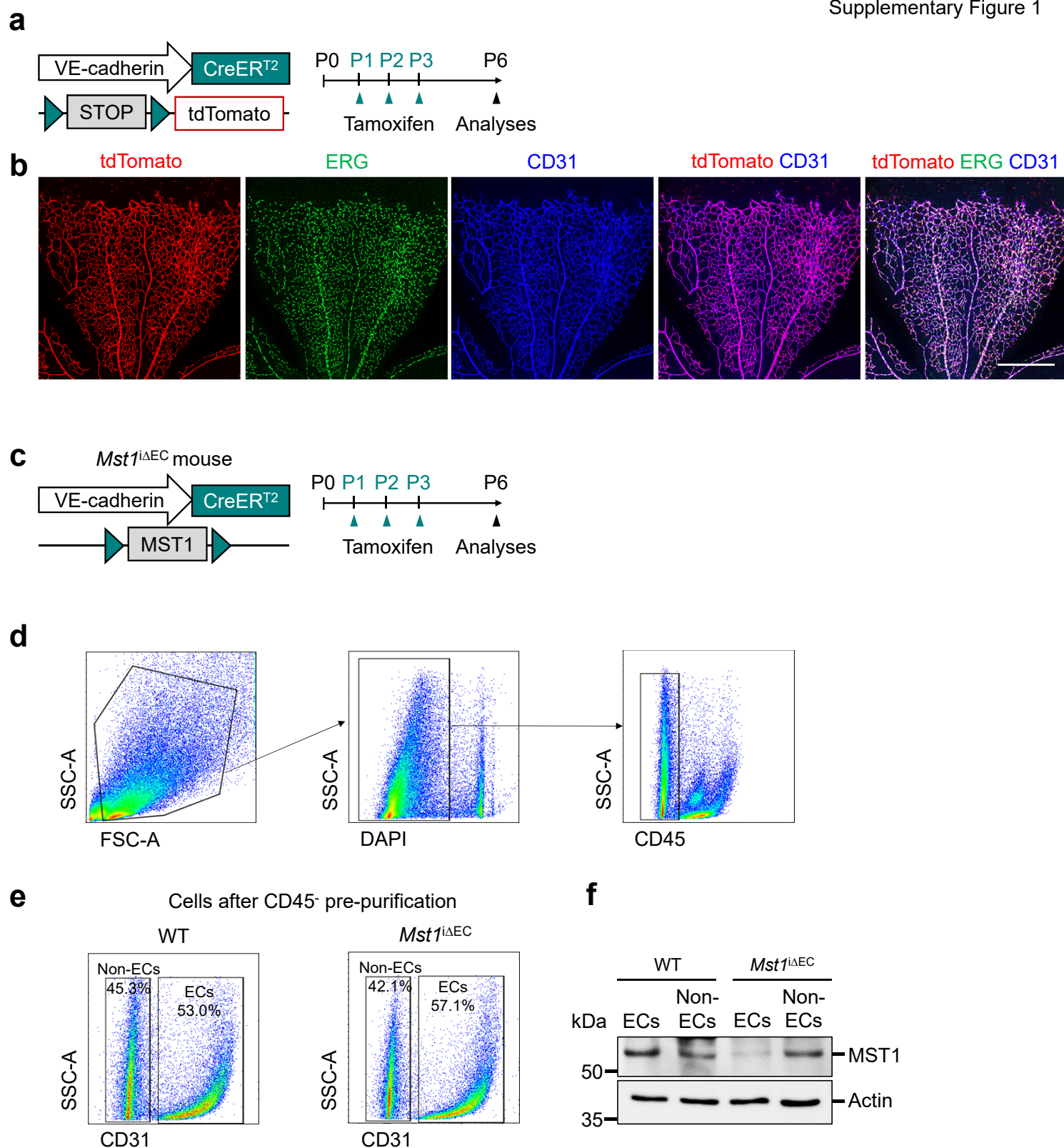
## Supplementary Information

### **A MST1-FOXO1 cascade establishes endothelial tip cell polarity and facilitates sprouting angiogenesis**

Yoo Hyung Kim, Jeongwoon Choi, Myung Jin Yang, Seon Pyo Hong, Choong-kun Lee, Yoshiaki Kubota, Dae-Sik Lim, Gou Young Koh

It includes;

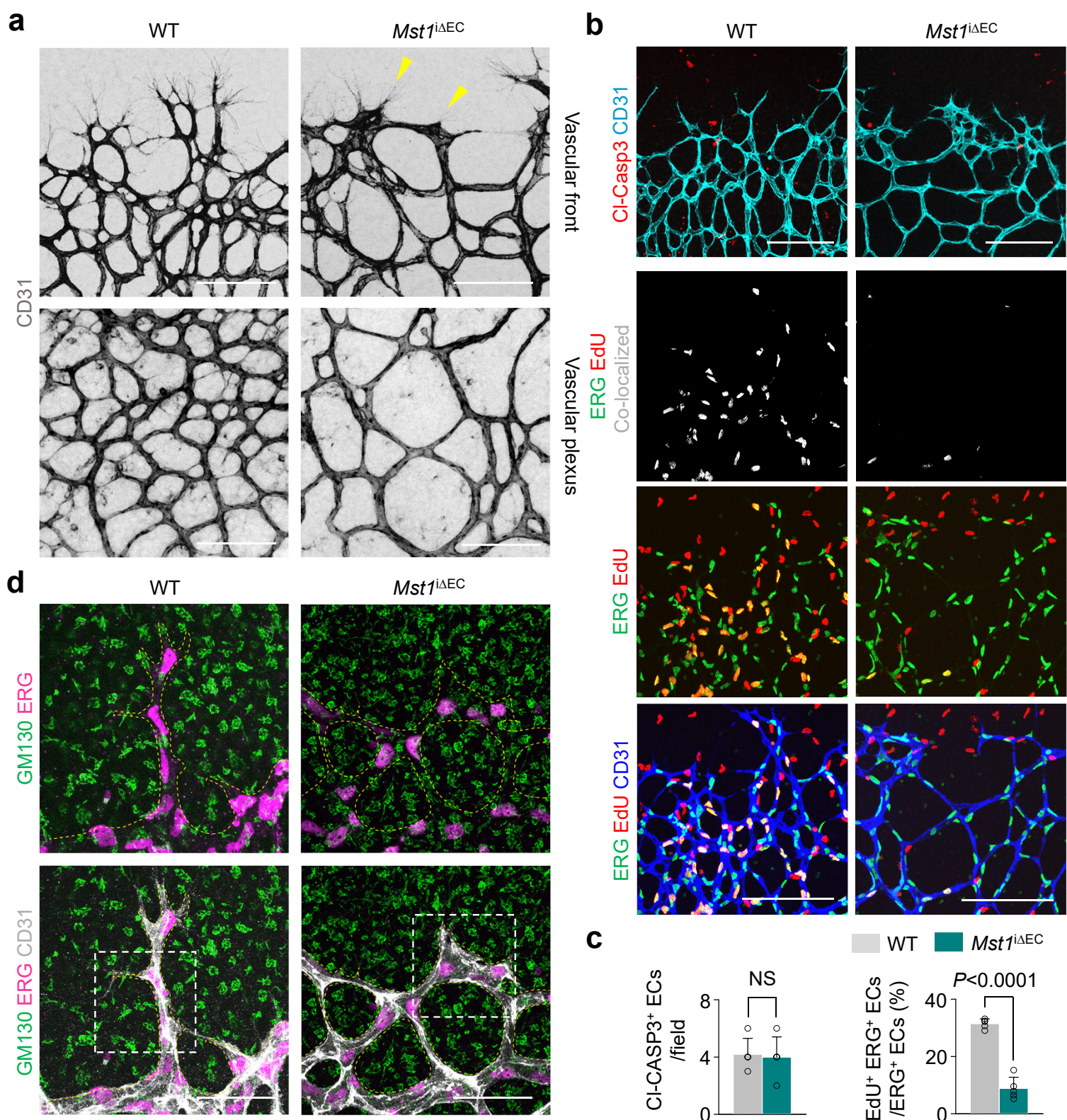
1. Supplementary Figures 1-11 and their legends
2. Supplementary Table 1.



### Supplementary Figure 1. Inducible EC-specific MST1 deletion in *Mst1*<sup>ΔEC</sup> mice.

(a) Diagram depicting the experimental schedule for monitoring EC-specific cre recombination using reporter mice with *VE-cadherin* Cre-ER<sup>T2</sup> mice. (b) Images of tdTomato, ERG<sup>+</sup> nuclei of EC and CD31<sup>+</sup> retinal vessels. Scale bars, 500  $\mu$ m. (c) Diagram depicting the experimental schedule for EC-specific deletion of MST1 in mouse lung ECs. (d) Gating strategy to sort CD45<sup>-</sup> cells from WT and *Mst1*<sup>ΔEC</sup> mice. (e) Gating strategy to sort Non-ECs (CD45<sup>-</sup>CD31<sup>-</sup>) and ECs (CD45<sup>-</sup>CD31<sup>+</sup>) from WT and *Mst1*<sup>ΔEC</sup> mice. Numbers above and inside of bracketed lines indicate percentages of cells. (f) Immunoblot analyses of indicated proteins in sorted ECs and Non-ECs of WT and *Mst1*<sup>ΔEC</sup> mice. Source data are provided as a Source Data file.

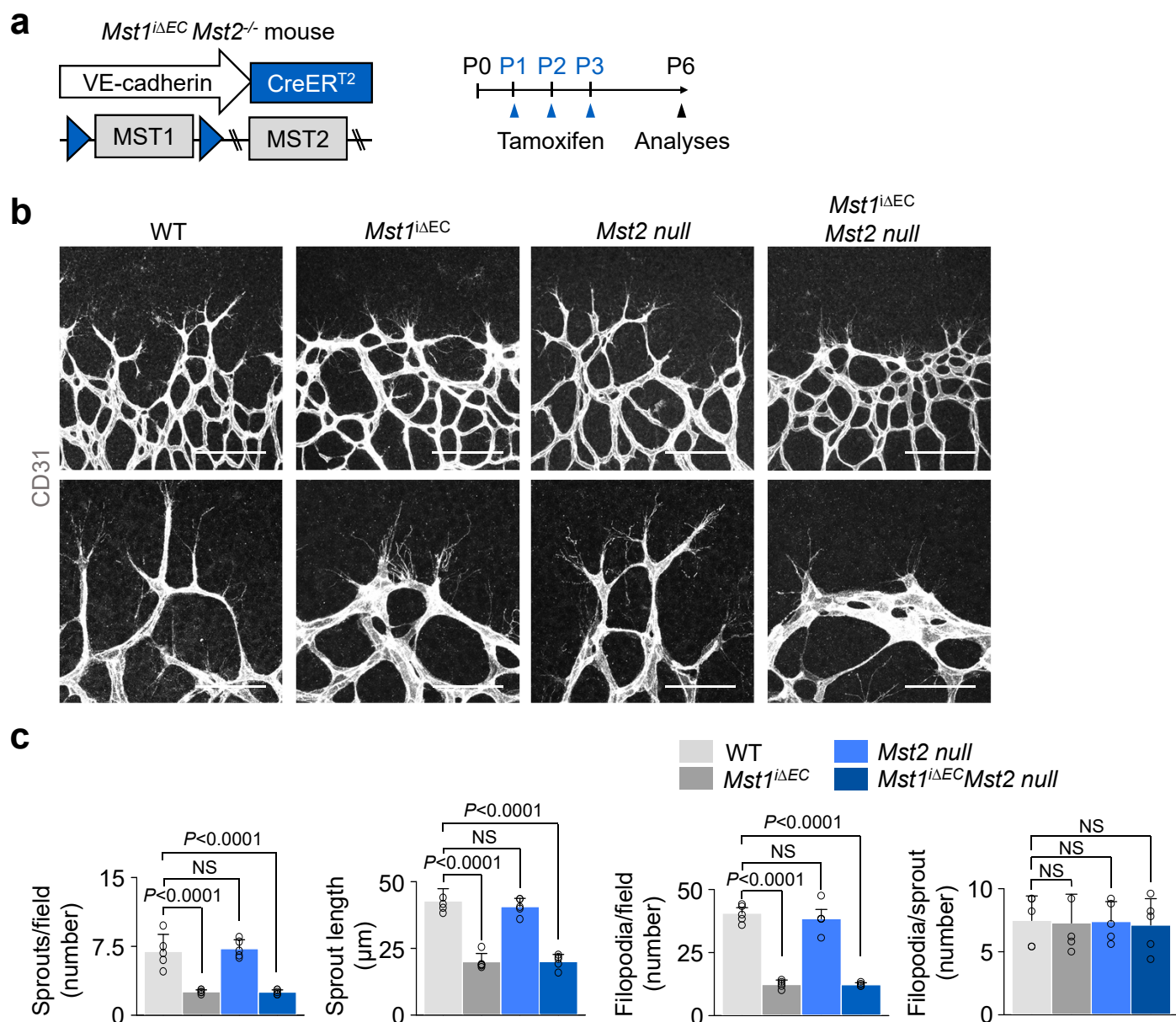




### Supplementary Figure 2. Endothelial MST1 deletion impairs EC proliferation and polarization.

(a) Representative images of retinal vessels in the vascular front and plexus of WT and *Mst1<sup>ΔEC</sup>* mice. Note that *Mst1<sup>ΔEC</sup>* mice exhibit shortened sprouts (yellow arrowheads) with reduced vascular density and branching. Scale bars, 100  $\mu$ m. (b, c) Images and comparisons of CI-CASP3<sup>+</sup> apoptotic ECs and EdU incorporated proliferating ECs in CD31<sup>+</sup> vessels of WT (n=5) and *Mst1<sup>ΔEC</sup>* (n=5) mice. Scale bars, 100  $\mu$ m. Data represent mean (bar)  $\pm$  s.d. (error bars). *P* values, versus WT by two-tailed unpaired *t*-test. NS, not significant. (d) Images of CD31<sup>+</sup> vessels, ERG<sup>+</sup> nuclei of ECs and GM130<sup>+</sup> Golgi apparatus at tip ECs of WT and *Mst1<sup>ΔEC</sup>* mice. The images of the insets (white dashed-line boxed) are magnified in Figure 1h. The yellow dashed line outlines CD31<sup>+</sup> vessels. Scale bars, 50  $\mu$ m. Source data are provided as a Source Data file.

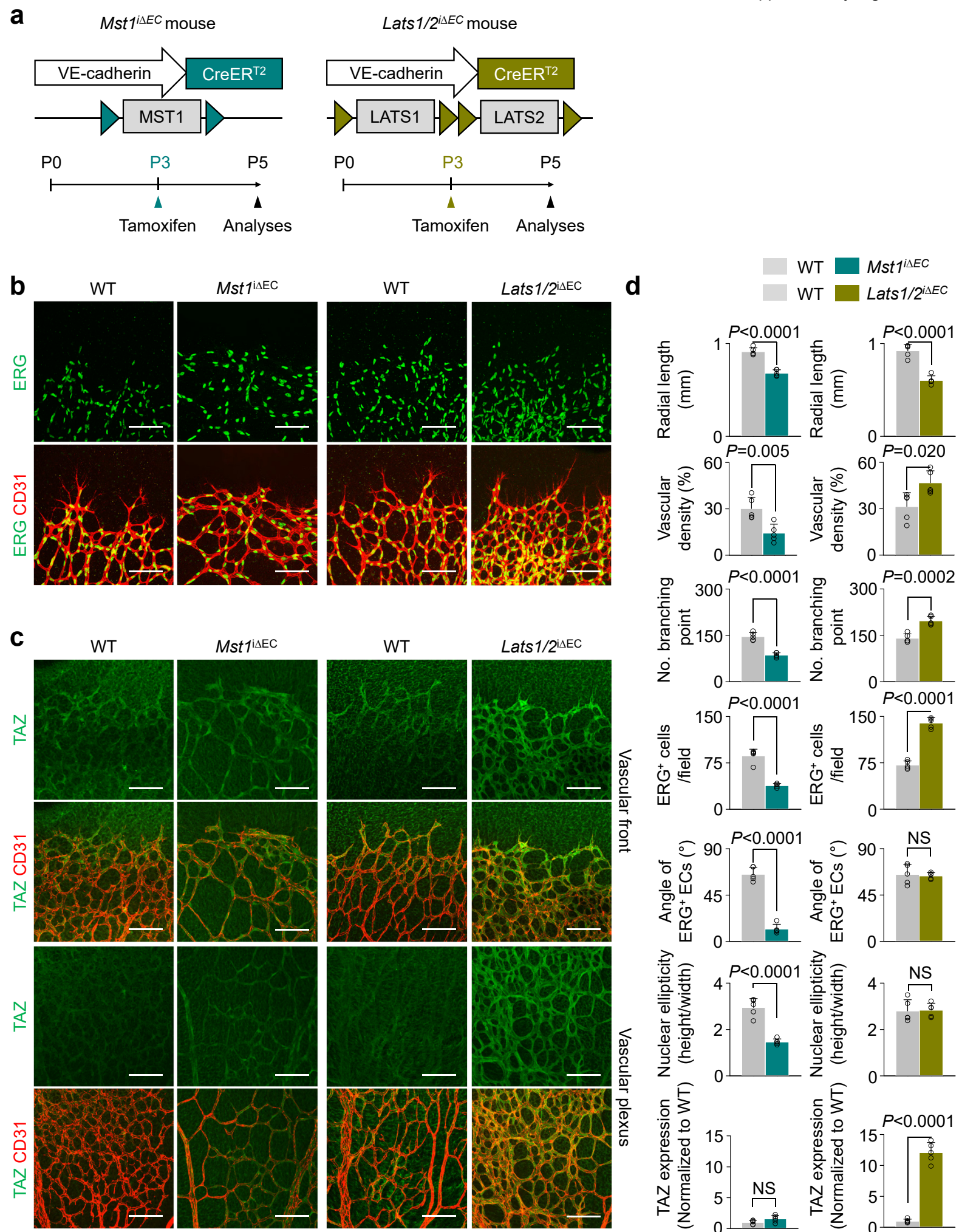




### Supplementary Figure 3. Endothelial MST1 but not MST2 is critical in sprouting angiogenesis.

(a) Diagram depicting the experimental schedule for EC-specific deletion of MST1 in retinal vessels from P1 and/or constitutive knockout of MST2 and their analyses at P6. (b, c) Images of CD31<sup>+</sup> vessels and comparisons of indicated parameters. Scale bars, 100 μm (upper panels); 50 μm (lower panels). Data represent mean (bar) ± s.d. (error bars). *P* values, versus WT NS, not significant. Source data are provided as a Source Data file.

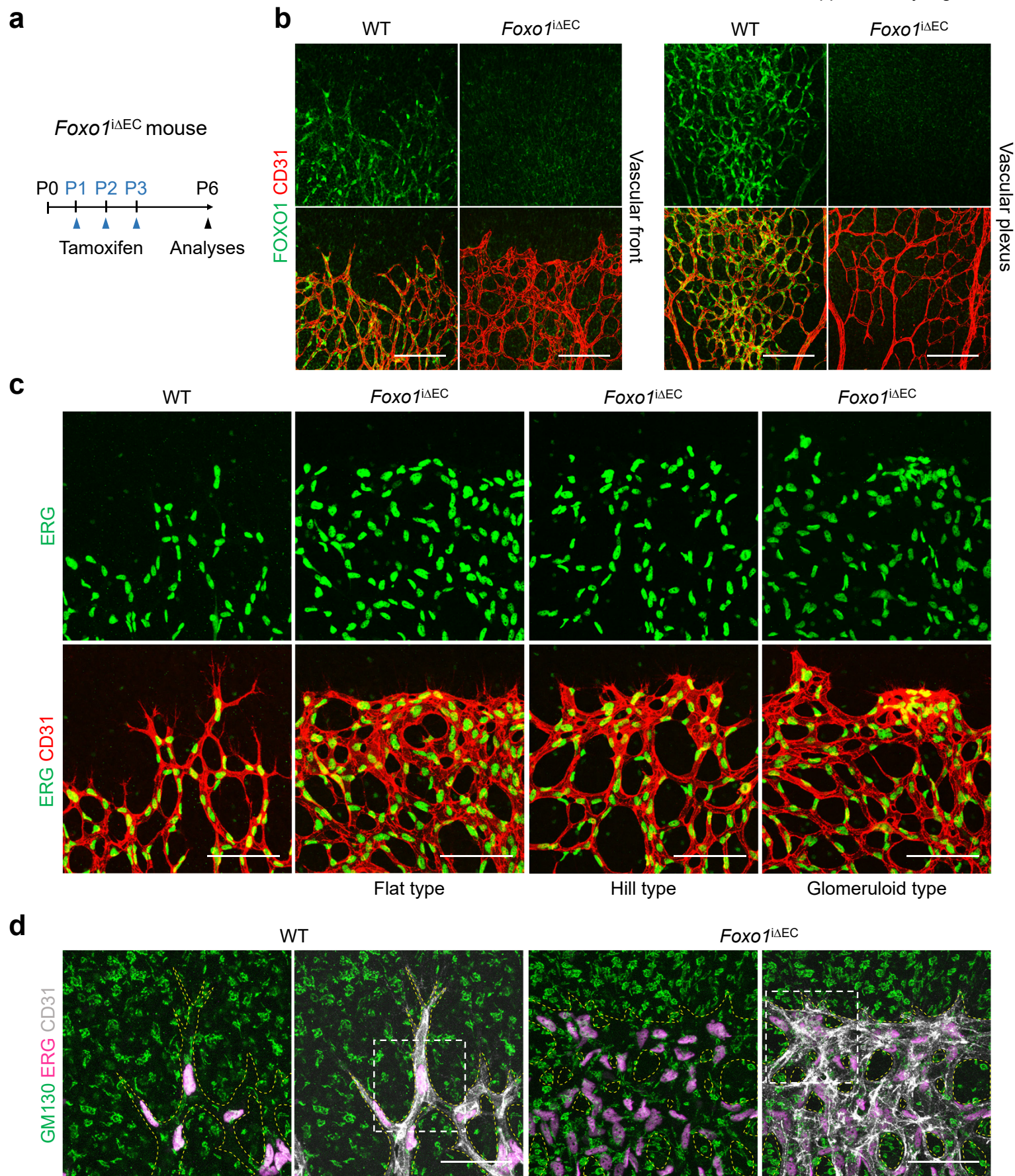




**Supplementary Figure 4. Endothelial MST1 does not rely on the canonical Hippo pathway for sprouting angiogenesis.**

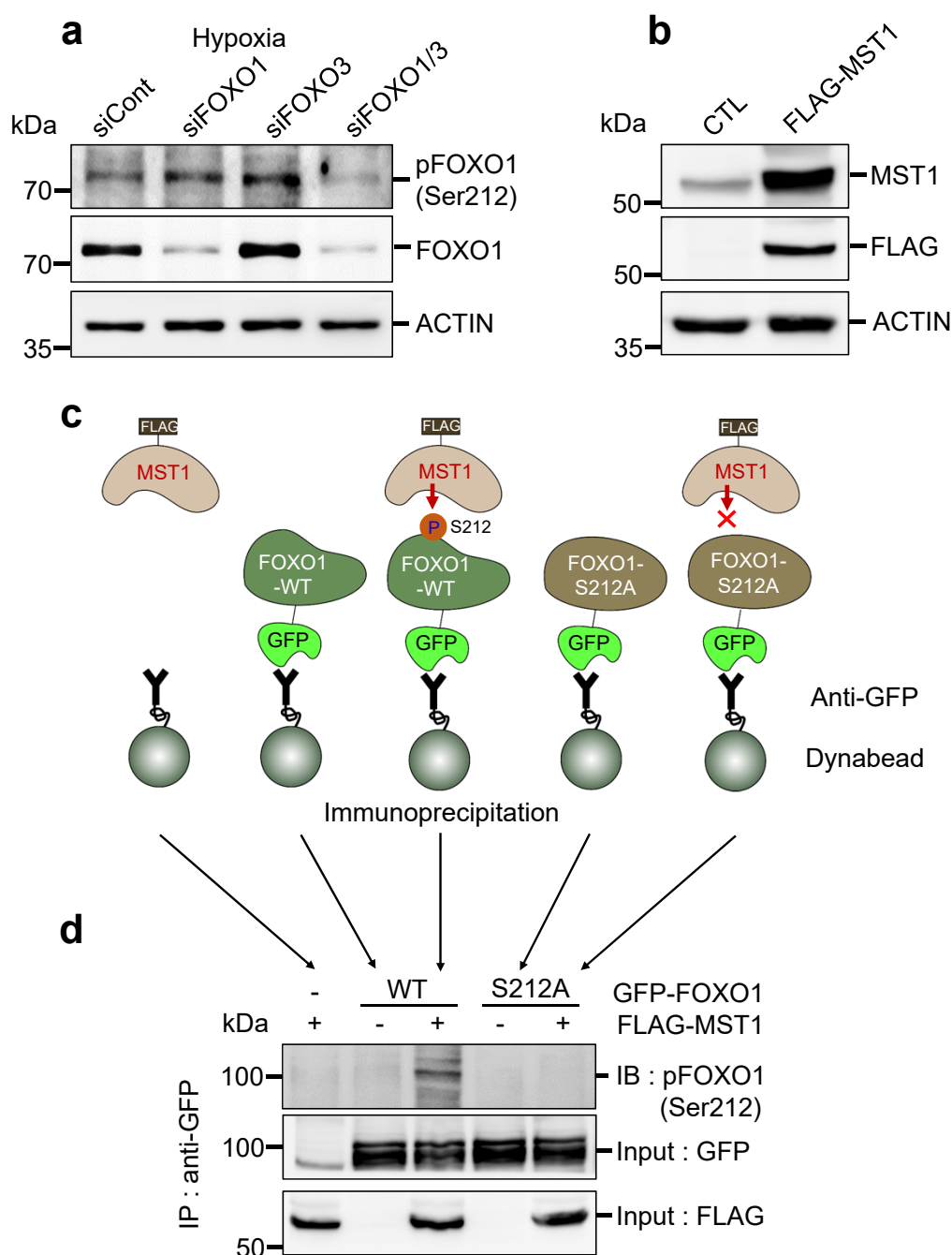
(a) Diagram depicting the experimental schedule for EC-specific deletion of MST1 or LATS1/2 in retinal vessels from P3 and their analyses at P5. (b) Images of CD31<sup>+</sup> vessels and ERG<sup>+</sup> nuclei of ECs in WT, *Mst1*<sup>ΔEC</sup> and *Lats1/2*<sup>ΔEC</sup> mice. Scale bars, 100 μm. (c) Images of TAZ distribution in CD31<sup>+</sup> vessels at vascular front and plexus in WT, *Mst1*<sup>ΔEC</sup> and *Lats1/2*<sup>ΔEC</sup> mice. (d) Comparisons of indicated parameters in two of each WT (n=5), *Mst1*<sup>ΔEC</sup> (n=5), and *Lats1/2*<sup>ΔEC</sup> (n=5) mice. Data represent mean (bar) ± s.d. (error bars). *P* values, versus WT by two-tailed unpaired *t*-test. NS, not significant. Source data are provided as a Source Data file.





**Supplementary Figure 5. Endothelial FOXO1 deletion impairs tip EC polarization.**

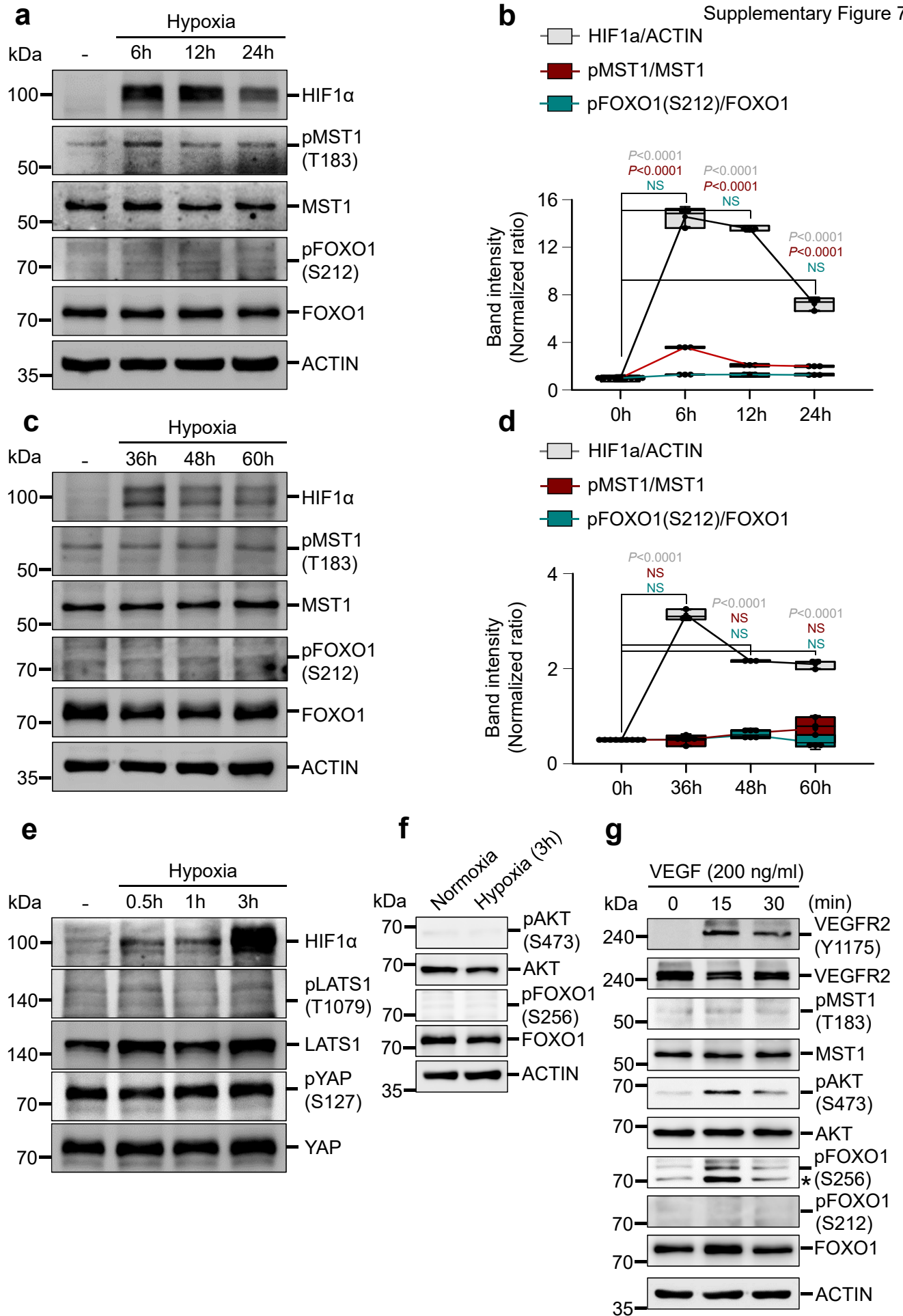
(a) Diagram depicting the experimental schedule for EC-specific deletion of FOXO1 in retinal vessels from P1 and their analyses at P6. (b) Images of FOXO1 distribution in CD31<sup>+</sup> vessels at P5 in WT and *Foxo1*<sup>ΔEC</sup> mice. Scale bars, 100 μm. (c) Images of CD31<sup>+</sup> vessels and ERG<sup>+</sup> nuclei of ECs showing variable sprouts morphology in *Foxo1*<sup>ΔEC</sup> mice. Scale bars, 50 μm. (d) Images of CD31<sup>+</sup> vessels, ERG<sup>+</sup> nuclei of ECs and GM130<sup>+</sup> Golgi apparatus at tip ECs of WT and *Foxo1*<sup>ΔEC</sup> mice. The images of the inset (white dashed-line boxed) are magnified in Figure 4g. The yellow dashed line outlines CD31<sup>+</sup> vessels. Scale bars, 50 μm.



**Supplementary Figure 6. The anti-phospho-FOXO1 polyclonal antibody recognizes FOXO1 phosphorylation at Serine 212.**

(a) Immunoblot analysis of indicated proteins in siCont-ECs, siFOXO1-ECs, siFOXO3-ECs (HUVECs transfected with siRNA targeting *FOXO3* gene) and siFOXO1/3-ECs for the validation of anti-phospho-FOXO1 (Ser212) antibody. (b) Immunoblot analysis of indicated proteins in HEK293T cells transfected with either control vector (CTL) or gene construct encoding MST1 (FLAG-MST1). (c) Schematic picture depicting our approach to validate anti-phospho-FOXO1 (Ser212) antibody. (d) Immunoprecipitation analysis in HEK293T cells with anti-GFP antibody followed by immunoblotting with anti-phospho-FOXO1 (Ser212) antibody. HEK293T cells were transfected with gene constructs encoding either GFP-tagged FOXO1 (GFP-FOXO1-WT) or non-phosphorylatable FOXO1 (GFP-FOXO1-S212A) together with either CTL or FLAG-MST1 prior to immunoprecipitation. Source data are provided as a Source Data file.

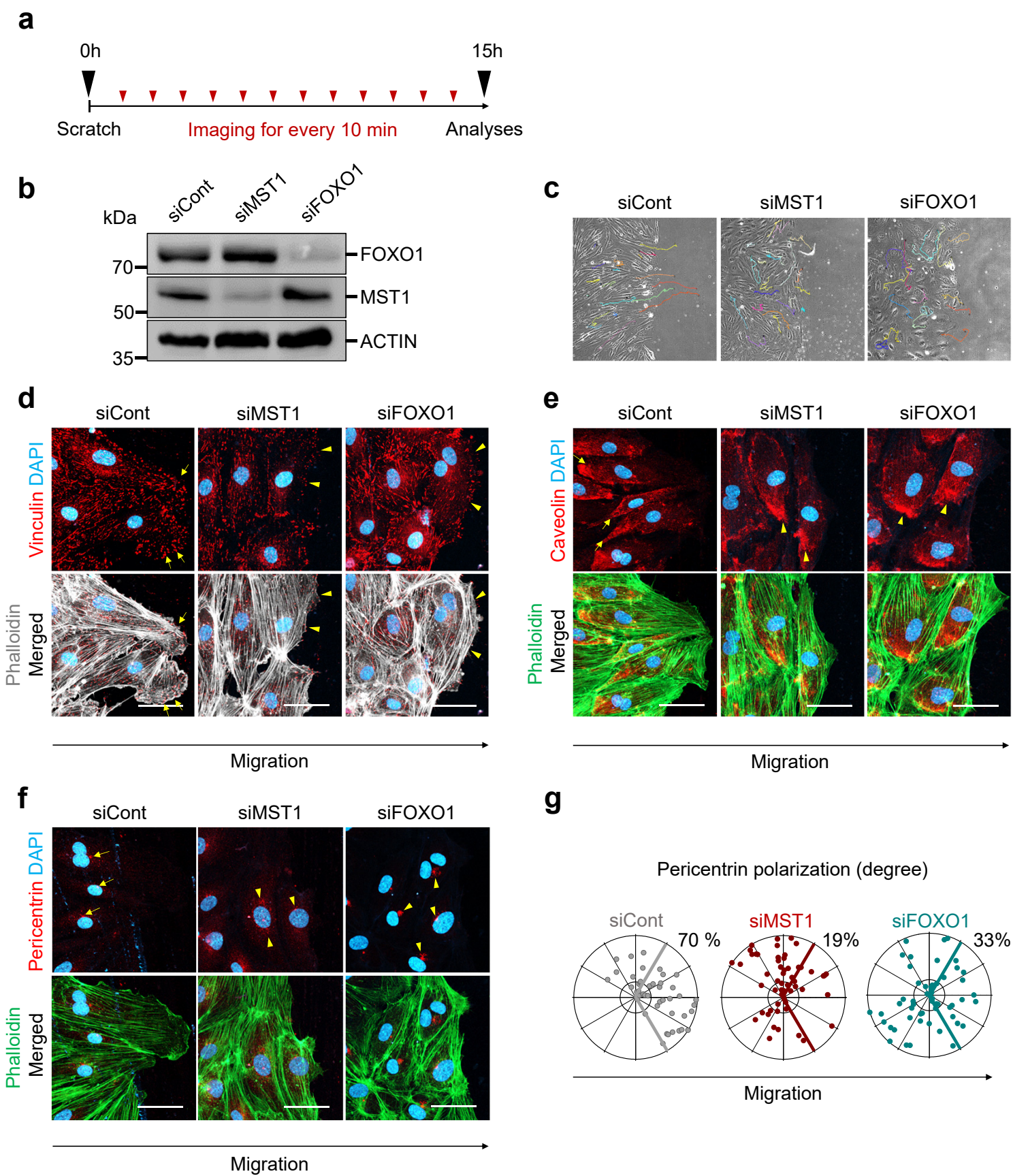




**Supplementary Figure 7. Hypoxia activates the MST1-FOXO1 cascade in primary cultured HUVECs**

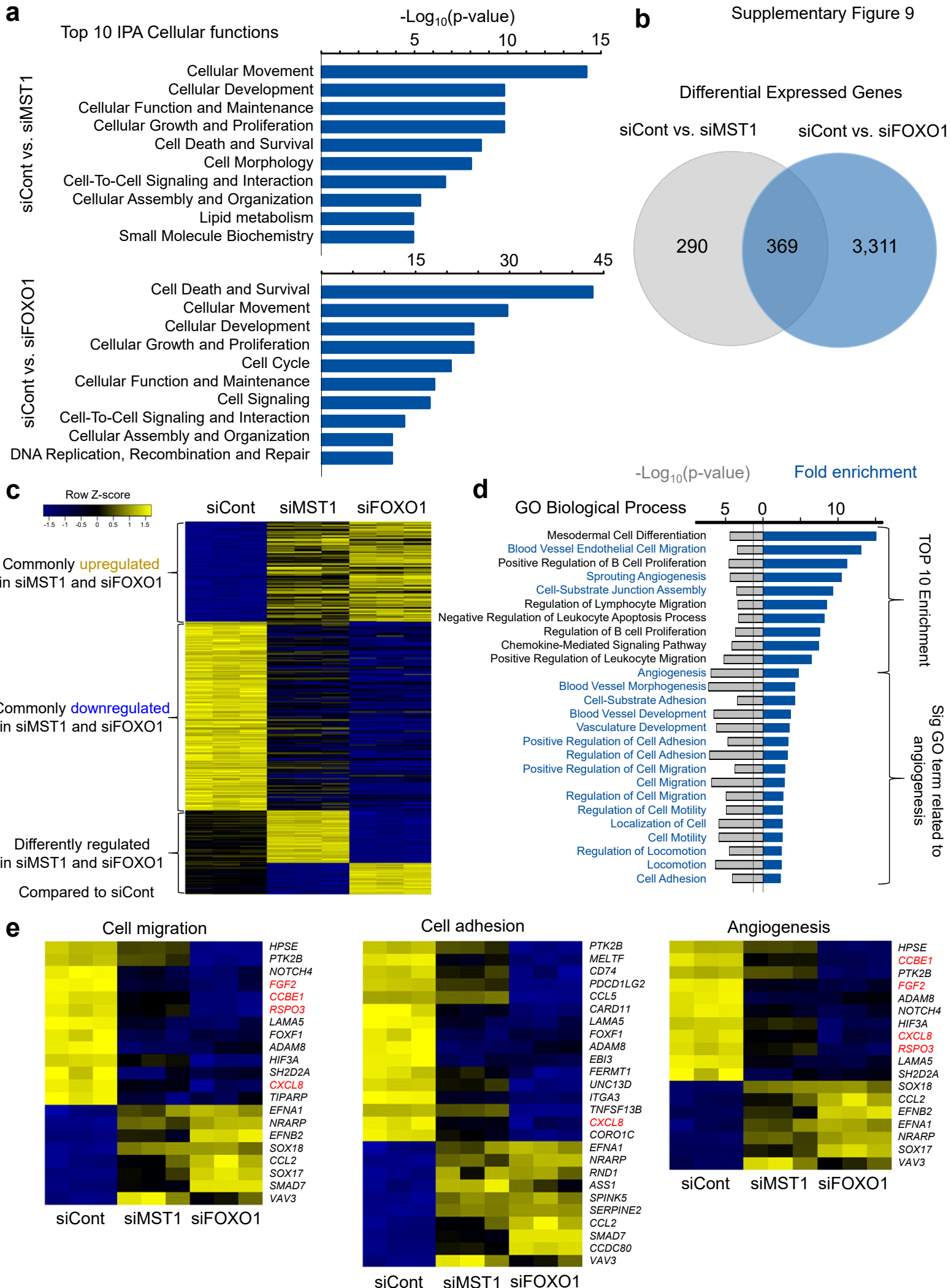
(a-d) Immunoblot analyses and comparisons of indicated proteins in HUVECs exposed to hypoxia (1% O<sub>2</sub>) for indicated times (n = 3, each group). Center line, median; Box limits, upper and lower quartiles; Whiskers, s.d. *P* values versus 0 h by one-way ANOVA with Tukey's *post hoc* test. NS, not significant. (e-g) Immunoblot analyses of indicated proteins in HUVECs exposed to hypoxia (1% O<sub>2</sub>) or VEGF (200 ng/ml) for indicated times. \*, nonspecific band.





**Supplementary Figure 8. MST1-FOXO1 cascade regulates cell polarity during directional EC migration**

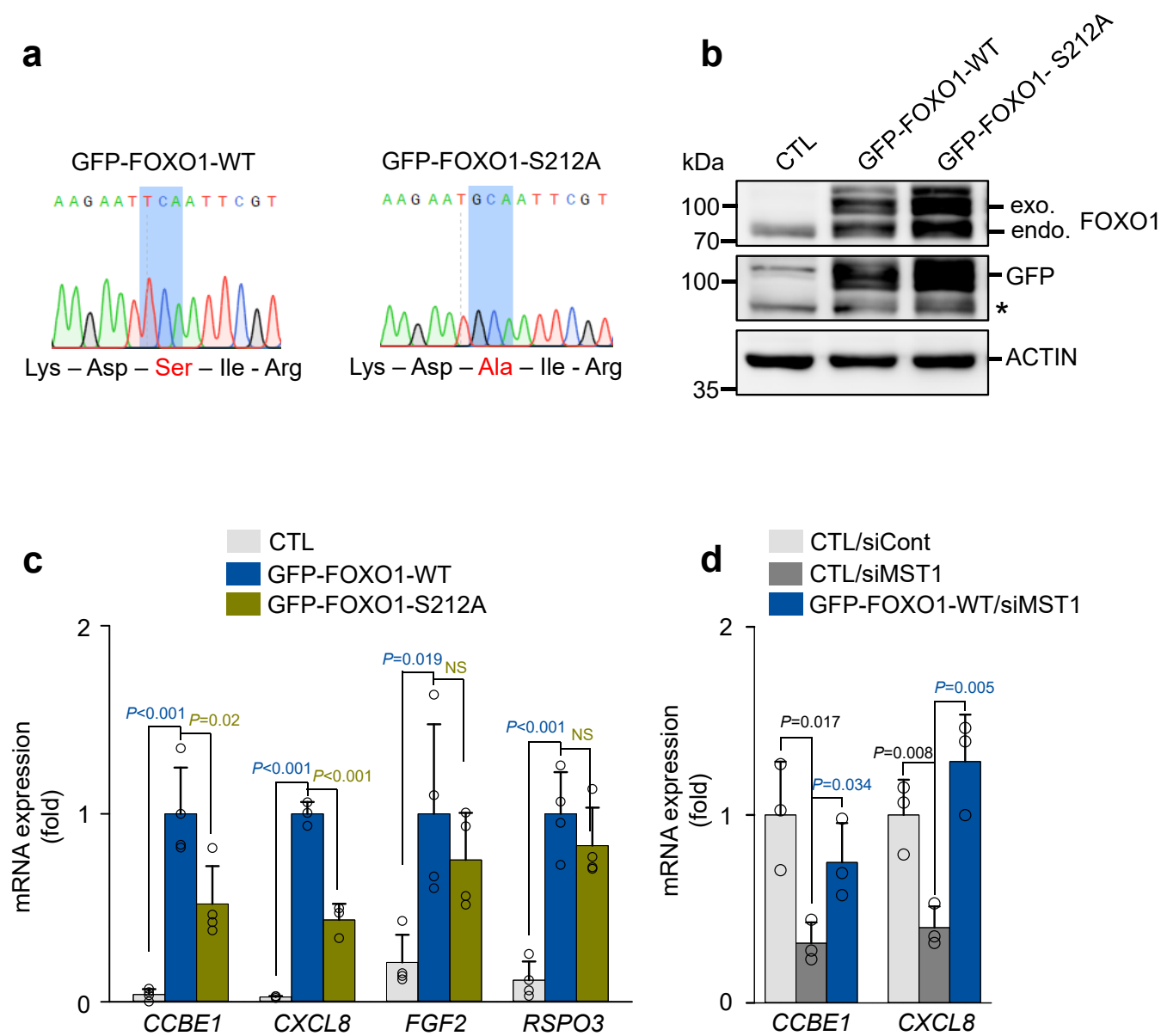
(a) Diagram depicting the experimental schedule for a wound scratch assay with time lapse imaging every 10 min for 15 h. (b) Immunoblot analyses in siCont-ECs, siMST1-ECs and siFOXO1-ECs to confirm depletion of the corresponding proteins. (c) Images of cell tracked line every 30 min in indicated ECs. n=19(siCont), 20(siMST1), 17(siFOXO1). Similar findings were observed in three independent experiments. (d) Representative images showing phalloidin<sup>+</sup> actin cytoskeleton, vinculin and DAPI in the leading edge of indicated ECs at 9 h after initiating cell migration. Note that vinculin incorporated focal adhesion (yellow arrowheads) and lamellipodia (yellow arrowheads) are rarely developed in siMST1-ECs and siFOXO1-ECs compared to siCont-ECs (yellow arrows). Scale bars, 50  $\mu$ m. (e) Representative images showing phalloidin<sup>+</sup> actin cytoskeleton, caveolin and DAPI in the leading edge of indicated ECs at 9 h after initiating cell migration. Note that caveolin (yellow arrows) in siCont-ECs are localized in the opposite direction of cell migration, while caveolin (yellow arrowheads) in siMST1-ECs and siFOXO1-ECs are localized randomly. Scale bars, 50  $\mu$ m. (f) Representative images showing phalloidin<sup>+</sup> actin cytoskeleton, pericentrin<sup>+</sup> centrosome and DAPI in the leading edge of indicated ECs at 9 h after initiating cell migration. Note that pericentrin<sup>+</sup> centrosome (yellow arrows) in siCont-ECs are localized in the direction of cell migration, while pericentrin<sup>+</sup> centrosome (yellow arrowheads) in siMST1-ECs and siFOXO1-ECs are localized randomly. Scale bars, 50  $\mu$ m. (g) Polar plots showing pericentrin polarization. n=45(siCont), 57(siMST1), 54(siFOXO1). The bold lines indicate 120° region centered on the vector which is vertical to the scratch direction. The numbers indicate the frequency of dots within the 120° region of the bold line. Source data are provided as a Source Data file.





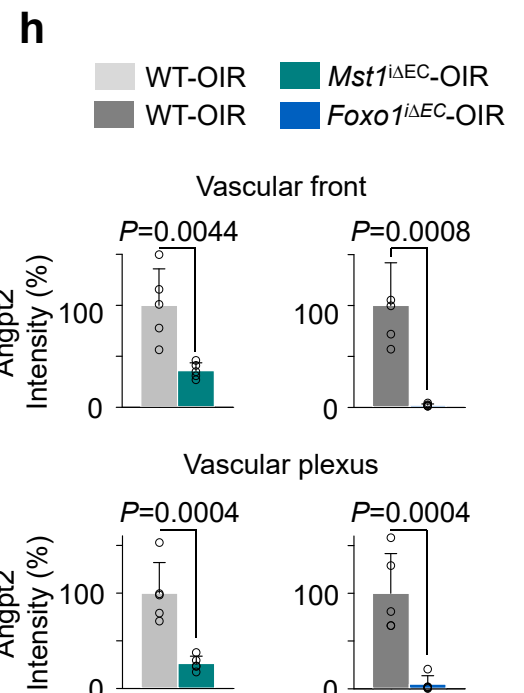
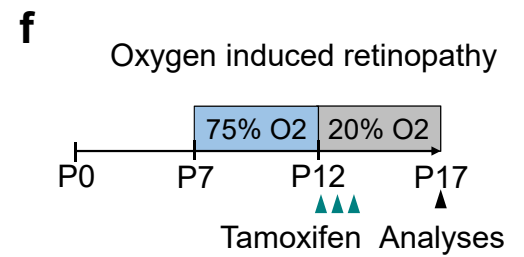
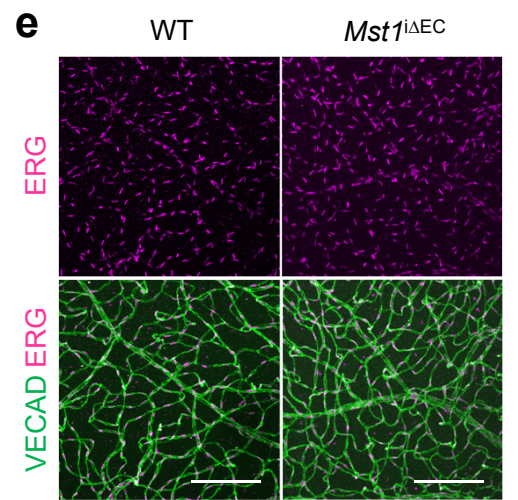
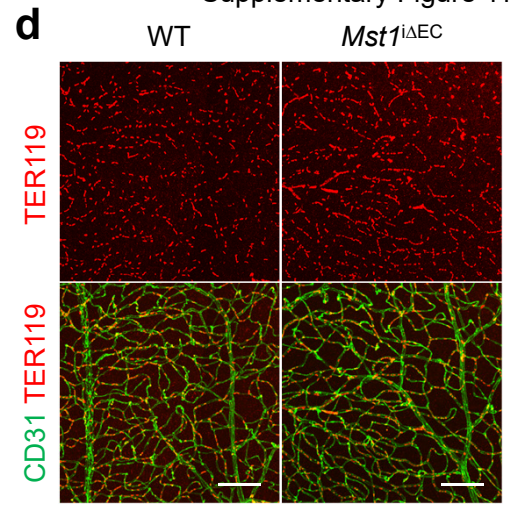
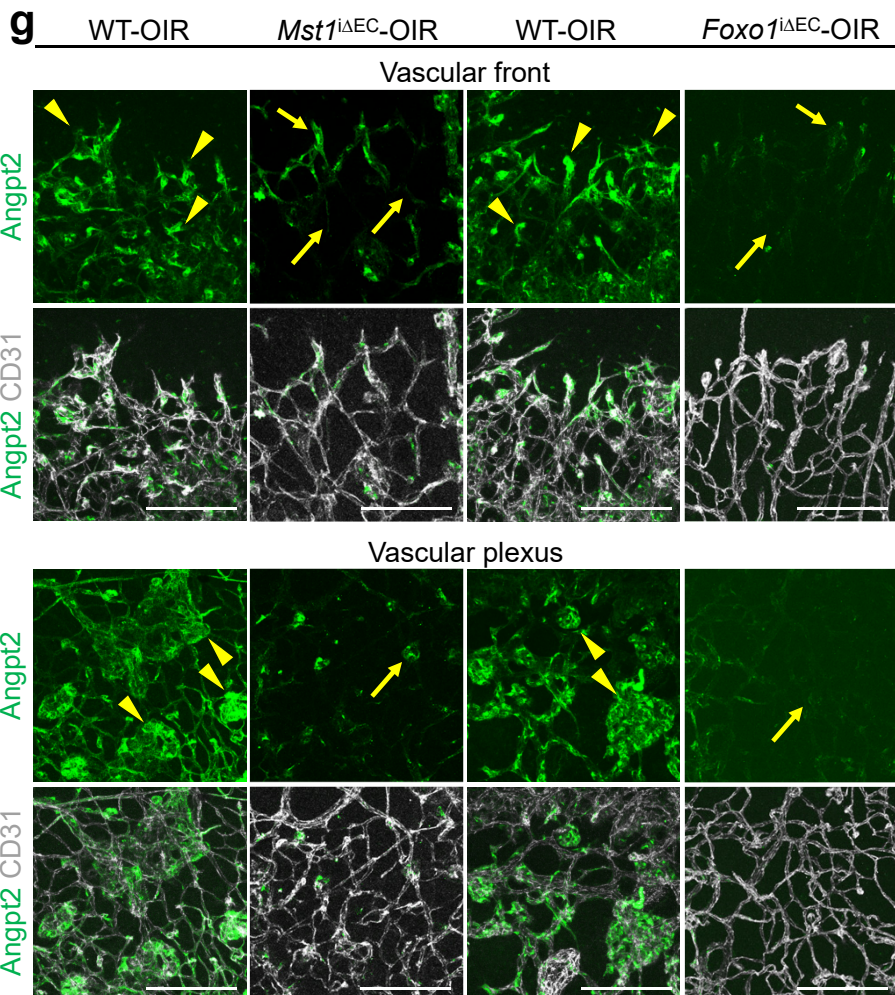
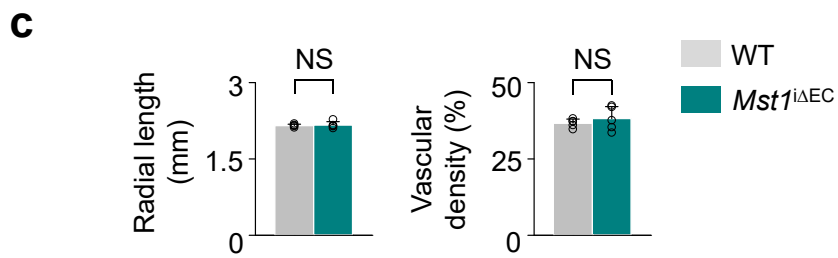
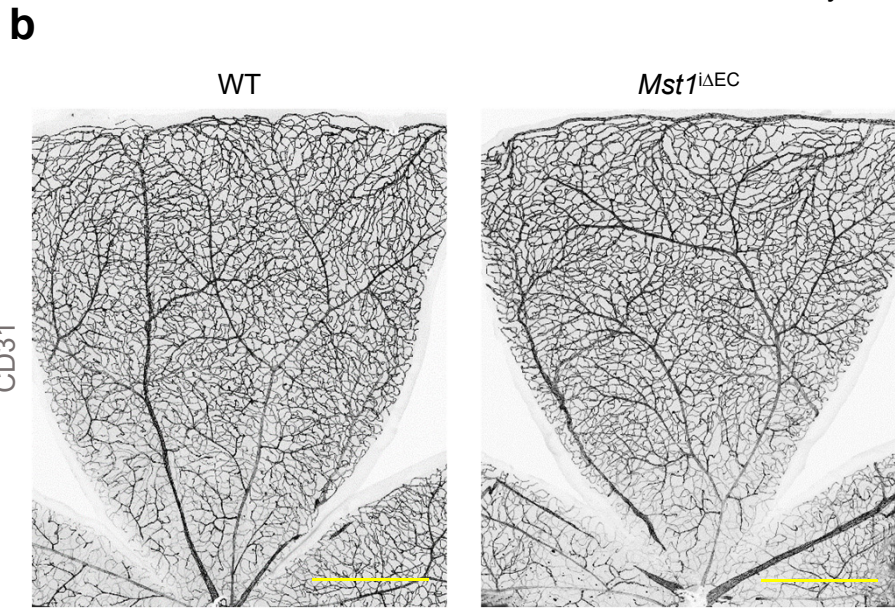
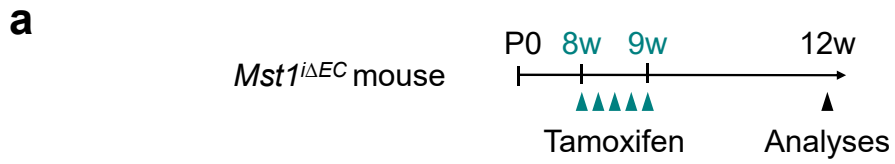
**Supplementary Figure 9. MST1-FOXO1 cascade regulates gene expression related to cell polarity.**

(a) Gene Ontology (GO) term analysis using IPA on the RNA sequencing data in comparison of siCont-ECs versus siMST1-ECs or siFOXO1-ECs (b) Venn-diagram depicting commonly regulated genes identified by differentially expressed gene analysis in siCont-ECs versus siMST1-ECs or siFOXO1-ECs. Numbers inside the Venn-diagram indicates the number of genes. (c) Clustered heat map of commonly regulated genes by MST1 and FOXO1. 286 of 369 genes are commonly up- or down regulated by MST1 and FOXO1. (d) GO term enrichment analysis for the commonly up- or down regulated genes by MST1 and FOXO1. False discovery rate  $\leq 0.05$ . (e) Representative clustered heat map of 'Cell migration', 'Cell adhesion' and 'Angiogenesis'. Genes marked in red are those with high fold change compared with siCont-ECs.



**Supplementary Figure 10. MST1-FOXO1 cascade transcriptionally regulates the expressions of *CCBE1* and *CXCL8*.**

(a) Diagram depicting DNA and protein sequences of gene constructs encoding FOXO1 (GFP-FOXO1-WT) and non-phosphorylatable FOXO1 (GFP-FOXO1-S212A). (b) Immunoblot analysis of indicated proteins in HUVECs transfected with gene constructs of control (CTL), GFP-FOXO1-WT, or GFP-FOXO1-S212A. \*, nonspecific band. (c) Quantitative PCR analyses of indicated gene expressions in HUVECs transfected with gene constructs of CTL, GFP-FOXO1-WT, or GFP-FOXO1-S212A. Data represent mean (bar)  $\pm$  s.d. (error bars). *P* values (blue), CTL versus GFP-FOXO1-WT by one-way ANOVA with Tukey's *post hoc* test. *P* values (green), GFP-FOXO1-WT versus GFP-FOXO1-S212A by one-way ANOVA with Tukey's *post hoc* test. (d) Quantitative PCR analyses of *CCBE1* and *CXCL8* gene expression in siCont-ECs transfected with gene constructs of CTL or siMST1-ECs transfected with gene constructs of CTL or GFP-FOXO1-WT. Data represent mean (bar)  $\pm$  s.d. (error bars). *P* values (black), CTL/siCont versus CTL/siMST1 by one-way ANOVA with Tukey's *post hoc* test. *P* values (blue), CTL/siMST1 versus GFP-FOXO1-WT/siMST1 by one-way ANOVA with Tukey's *post hoc* test. NS, not significant. Source data are provided as a Source Data file.





**Supplementary Figure 11. Endothelial MST1 is dispensable for vessel maintenance, but MST1-FOXO1 cascade is required for pathological angiogenesis.**

(a) Diagram depicting the experimental schedule for EC-specific deletion of MST1 in retinal vessels of 8-week-old mice and their analysis after 4 weeks in *Mst1<sup>iΔEC</sup>* mice. (b, c) Images of CD31<sup>+</sup> retinal vessels and comparisons of indicated parameters in WT (n=5) and *Mst1<sup>iΔEC</sup>* (n=5) mice. Scale bars, 500 μm. (d) Images of TER119<sup>+</sup> RBC and CD31<sup>+</sup> vessels. No visible hemorrhage is detected in both mice. Scale bars, 100 μm. (e) Images of VECAD and ERG<sup>+</sup> nuclei of ECs. No abnormal alignment of ECs nuclei is observed in both mice. Scale bars, 100 μm. (f) Diagram depicting the experimental schedule for generation of oxygen-induced retinopathy model (OIR) in WT, *Mst1<sup>iΔEC</sup>*, and *Foxo1<sup>iΔEC</sup>* mice. (g, h) Images of CD31<sup>+</sup> vessels and Angpt2 expression and comparisons of Angpt2 intensity in tip ECs and NVT ECs in WT-OIR (n=5), *Mst1<sup>iΔEC</sup>*-OIR (n=5), and *Foxo1<sup>iΔEC</sup>*-OIR (n=5) mice. Note that Angpt2 expression is reduced in tip ECs and NVT ECs in *Mst1<sup>iΔEC</sup>*-OIR and *Foxo1<sup>iΔEC</sup>*-OIR (yellow arrows) compared with that in WT-OIR mice (yellow arrowheads). Scale bars, 100 μm. Data represent mean (bar) ± s.d. (error bars). *P* values, versus WT by two-tailed unpaired *t*-test. Source data are provided as a Source Data file.

**Supplementary Table 1. List of Primer Sets for Quantitative Real-Time RT-PCR for human samples**

Name	Sequence (5' - 3')	
<i>CCBE1</i>	Forward	CACATTAAGCAAGGCCGGAG
	Reverse	TCCTCTCTCCCCCTTAGAACC
<i>CXCL8</i>	Forward	CATACTCCAAACCTTTCCACC
	Reverse	AGCTTTACAATAATTTCTGTGTTGG
<i>FGF2</i>	Forward	TGGTATGTGGCACTGAAACG
	Reverse	TATAGCTTTCTGCCCAGGTCC
<i>RSPO3</i>	Forward	ACAATTGCCCAGAAGGGTTG
	Reverse	AGTCCCTCTTTTGAAGCCAC
<i>GAPDH</i>	Forward	CCACTCCTCCACCTTTGACG
	Reverse	TTCGTTGTCATACCAGGAAATGAG